

The influence of coronal EUV irradiance on the emission in the He I 10830 Å and D₃ multiplets

R. Centeno^{1,2}, J. Trujillo Bueno^{1,3}, H. Uitenbroek⁴ and M. Collados¹

rce@ucar.edu, jtb@iac.es, huitenbr@nso.edu, mcv@iac.es

ABSTRACT

Two of the most attractive spectral windows for spectropolarimetric investigations of the physical properties of the plasma structures in the solar chromosphere and corona are the ones provided by the spectral lines of the He I 10830 Å and 5876 Å (or D₃) multiplets, whose polarization signals are sensitive to the Hanle and Zeeman effects. However, in order to be able to carry out reliable diagnostics, it is crucial to have a good physical understanding of the sensitivity of the observed spectral line radiation to the various competing driving mechanisms. Here we report a series of off-the-limb non-LTE calculations of the He I D₃ and 10830 Å emission profiles, focusing our investigation on their sensitivity to the EUV coronal irradiation and the model atmosphere used in the calculations. We show in particular that the intensity ratio of the blue to the red components in the emission profiles of the He I 10830 Å multiplet turns out to be a good candidate as a diagnostic tool for the coronal irradiance. Measurements of this observable as a function of the distance to the limb and its confrontation with radiative transfer modeling might give us valuable information on the physical properties of the solar atmosphere and on the amount of EUV radiation at relevant wavelengths penetrating the chromosphere from above.

Subject headings: Radiative transfer, line: formation, Sun: chromosphere, Sun: UV radiation

¹Instituto de Astrofísica de Canarias, 38205 La Laguna, Tenerife, Spain

²High Altitude Observatory (NCAR), Boulder CO 80301, USA

³Consejo Superior de Investigaciones Científicas (Spain)

⁴National Solar Observatory, Sac. Peak, NM, USA

1. Introduction

The spectral lines of the multiplet of neutral helium at 10830 Å are of great diagnostic value for investigating the dynamic and magnetic properties of plasma structures in the solar chromosphere and corona. This is because their polarization is sensitive to the presence of atomic level polarization and to the joint action of the Hanle and Zeeman effects (e.g. Trujillo Bueno & Asensio Ramos, 2007), which makes these lines especially sensitive to the strongest fields found in solar active regions (e.g., Harvey & Hall 1977; Rüedi et al. 1995; Centeno et al. 2006) and also to the weaker fields encountered in a variety of plasma structures such as filaments (e.g., Lin et al. 1998; Trujillo Bueno et al. 2002), regions of emerging magnetic flux (e.g., Lagg et al. 2004), chromospheric spicules (e.g., Trujillo Bueno et al. 2005; Socas-Navarro et al. 2005) and prominences (e.g., Merenda et al. 2006). Obviously, in order to be able to obtain reliable inferences from the observed spectral line radiation it is necessary to reach a rigorous physical understanding of the key mechanisms that are responsible for its intensity and polarization. The same applies to the lines of the He I D₃ multiplet at 5876 Å whose observed polarization has been used for investigating the magnetic field vector in solar prominences and spicules (e.g., Landi Degl’Innocenti 1982; Leroy, Bommier & Sahal-Bréchet, 1983; Casini et al. 2003; López Ariste & Casini 2005; Bianda et al. 2006; Ramelli et al. 2006 a,b).

While the modeling of the spectral line intensity has been done by solving the standard non-LTE radiation transfer problem in one-dimensional (1-D) semi-empirical models of the solar atmosphere (e.g., Pozhalova 1988; Avrett et al. 1994; Andretta & Jones 1997), the physical interpretation of the observed spectral line polarization has been carried out taking into account the joint action of the Hanle and Zeeman effects within the framework of the quantum theory of polarization, but simplifying the radiative transfer problem by using the optically thin approximation (e.g., Landi Degl’Innocenti, 1982; Leroy et al, 1983; Casini et al 2004) or by solving the Stokes-vector transfer equation in a slab of constant physical properties (Trujillo Bueno et al. 2002; 2005).

In this slab model for the interpretation of polarization observations, the slab’s optical thickness is simply chosen as a free parameter to fit the observed intensity profile. This “cloud” model for the interpretation of polarization observations simplifies the forward modeling and inversion problem (see Trujillo Bueno & Asensio Ramos, 2007; Asensio Ramos & Trujillo Bueno 2007), but it does not give us information on the possible errors we make by not considering explicitly the physical mechanisms that are thought to be responsible for producing some optical thickness in such lines of neutral helium.

According to the above-mentioned non-LTE radiative transfer investigations in 1D semi-empirical models of the solar atmosphere there are two candidates for producing a significant

optical thickness in the lines of the 10830 Å and D₃ multiplets, given that the collisional excitations at typical solar chromospheric temperatures (<20000 K) are unable to significantly populate the triplet levels of He I. The first mechanism states that the EUV radiation irradiating the chromosphere ionizes part of the substantial amount of neutral helium atoms that are found in the ground singlet state at the typical chromospheric temperatures, which then lead to recombinations that produce an enhanced population of the triplet states (e.g., Pozhalova 1988; Avrett et al. 1994). The second one deals with the possibility of collisional excitation by a significant amount of transition region material at temperatures greater than 20000 K (e.g., Andretta & Jones 1997). In our opinion, as we shall try to show in this paper, detailed off-limb observations of the intensity and polarization profiles of the He I 10830 Å multiplet should help us determine which is the dominating mechanism, or if both are playing an equally significant role.

The mechanism of collisional excitation at temperatures greater than 20000 K seems to require (or is helped by) the existence of a temperature “plateau” located in the lower transition region (TR) of the Sun, such as that included ad-hoc by Vernazza et al. (1981) in their semi-empirical models in order to be able to model the observed Ly_α radiation. Interestingly enough, the consideration of ambipolar diffusion effects in such semi-empirical models led to a new series of models by Fontenla et al. (1990; 1991; 1993) that are able to explain the observed Ly_α intensity observations without the need of such a TR “plateau”. In this new series of semi-empirical models (FAL models), an enhanced population in the triplet states of He I can only be produced by the above mentioned Photoionization-Recombination process (hereafter: the PR mechanism).

The main aim of this paper is to investigate the sensitivity of the off-the-limb emission profiles of the 10830 Å and D₃ lines to the amount of coronal EUV radiation. To this end, we have chosen the above-mentioned FAL-like models and have solved the RT problem in spherical geometry for increasing values of the EUV coronal irradiance. As we shall see, this has allowed us to demonstrate that the intensity ratio of the blue and red components of the 10830 Å multiplet is a sensitive function of the amount of coronal EUV illumination, and to establish this very observable as an ideal candidate for mapping the amount of coronal EUV irradiance at more or less active off-limb locations and for determining whether or not the PR mechanism is truly the dominating one. We also show the variation of this intensity ratio with the atmospheric height when using an atmospheric model with a TR “plateau” in the model’s temperature profile. In our opinion, the comparison of this type of simulations with observations should allow us to determine whether there is any off-limb region of the Sun (e.g., above plages?) where collisional excitation plays a significant role in addition to the PR mechanism.

The outline of this paper is as follows. The formulation of the problem is presented in Sect. 2, where we describe our approach to model the off-limb emission profiles of the aforementioned multiplets. Section 3 focuses on the sensitivity of these profiles to the EUV coronal irradiation and points out the existence of an interesting observable (i.e., the above-mentioned intensity ratio) that can serve as diagnostic tool for this physical quantity. Finally, in section 4 we summarize the highlights and discuss possible lines of future research.

2. Formulation of the problem

For understanding the formation of these helium lines we carried out a series of non-LTE radiative transfer calculations of the off-limb intensity profiles emerging from various semi-empirical atmospheric models using a 1D spherically symmetric geometry version of the RH code (see <http://www.nso.edu/staff/uitenbr/rh.html>). This non-LTE radiative transfer code, based on the Multi-level Accelerated Lambda Iteration (MALI) scheme by Rybicki & Hummer (1991, 1992), solves the combined equations of statistical equilibrium and radiative transfer for a multilevel atom in a given stellar atmospheric model (see also Socas-Navarro and Trujillo Bueno, 1997). The code deals with overlapping transitions, and besides from the opacities and emissivities produced by the transitions in the *active* atom (the one that is considered in full non-LTE regime) it also accounts for background radiation due to other atoms, molecules and relevant continuum processes.

The calculations of the emergent emission spectra were done in the context of the FAL model atmospheres (Fontenla et al, 1990, 1991, 1993), which require the above-mentioned PR mechanism for producing significant off-limb emission in the He I 10830 Å and D_3 multiplets. We have used these semi-empirical models as tabulated (i.e. without considering any possible feedback effect of the EUV irradiance on the models themselves). The main analysis is carried out with the FAL-C model of the average quiet Sun, although a comparison of the results among FAL-C, FAL-P (representative of a plage region) and the M_{CO} model of Avrett (i.e., the relatively cool M_{CO} model atmosphere illustrative of the quiet Sun that Avrett (1995) proposed to account for the observed molecular CO absorption at 4.6 μm) is described at the end of section 3. In addition, we show also a comparison with the results obtained in the VAL-C model of Vernazza et al. (1981), whose temperature plateau (with $T > 20000$ K) in its TR to the coronal gas, gives rise to a localized collisional enhancement of the triplet states populations.

The atomic model of He that we used (see Fig. 1) accounts for 165 possible bound-bound transitions taking place among 53 energy levels (46 of He I, 6 of He II and 1 of He III). The fine structure of the triplet energy levels was taken into account, together with all

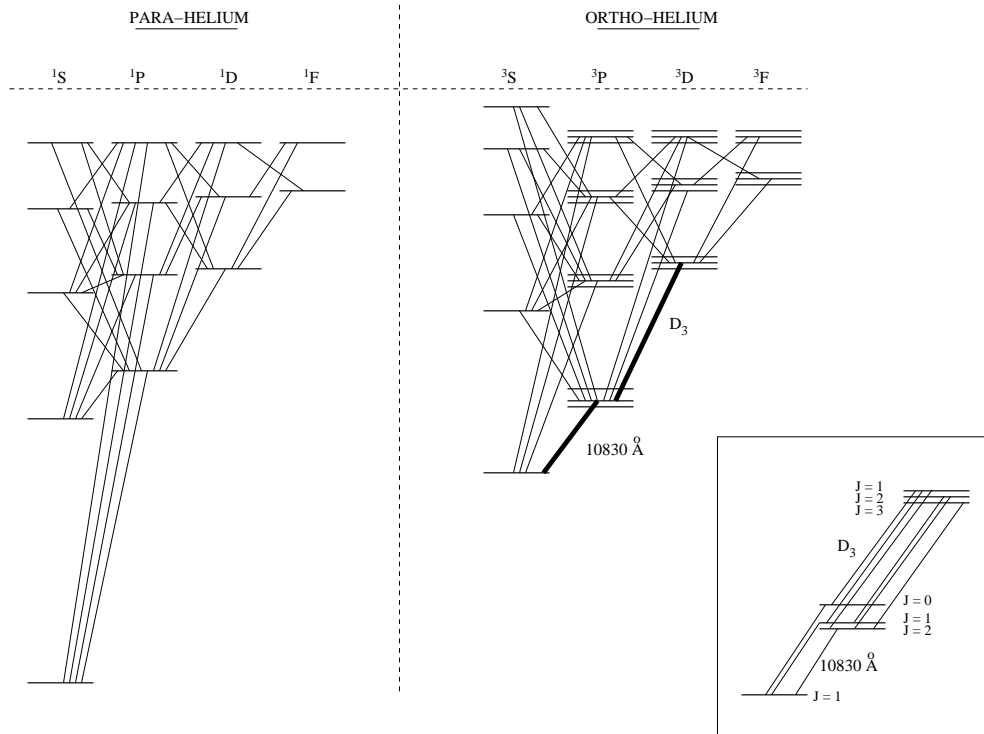


Fig. 1.— Schematic atomic model of He I, with 46 energy levels and the transitions between each pair of levels. Although the multiple transitions among triplet levels are not represented in the figure, they were taken into account in the calculations. The individual He I 10830 Å and D_3 transitions are highlighted in the inset.

the possible combinations of transitions between them. The radiative transition parameters were obtained from the NIST database¹ and the collisional rate coefficients were calculated using the Seaton (1962) impact approximation for neutral bound-bound and the Van Regemorter’s (1962) approximation for treating bound-bound transitions caused by collisions with electrons. Both photoionization and collisional ionization bound-free cross-sections are also tabulated in the atomic model file and were extracted from Landolt-Börnstein (1982).

Despite its simplicity from the atomic point of view, the atom of Helium shows quite a complicated spectrum with two different spectral series: one of singlets (Para-Helium) involving singlet terms (1S , 1P , 1D ..) and the other one of triplets (Ortho-Helium) involving triplet terms (3S , 3P , 3D ..). In the electric dipole approximation, quantum selection rules do not allow radiative transitions between singlet and triplet terms, so the populations of

¹National Institute for Standards and Technology, see <http://physics.nist.gov/PhysRefData/ASD/index.html>

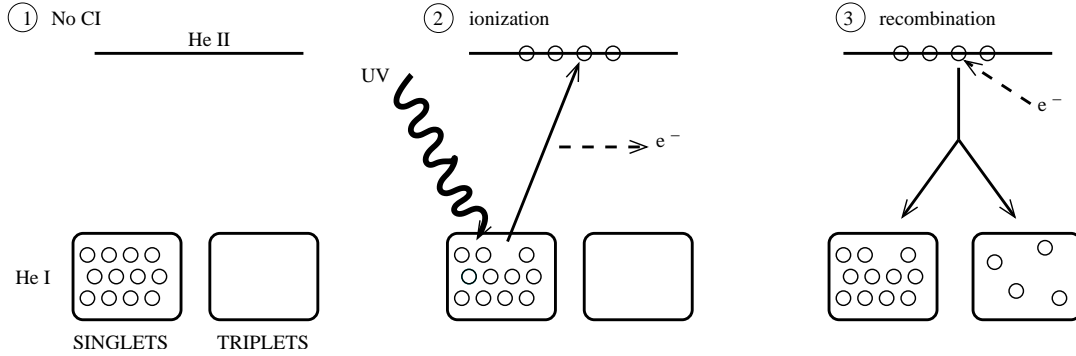


Fig. 2.— Ionization-recombination scheme for the He atom triggered by the EUV coronal irradiance (CI). In the absence of CI (panel 1) nearly all the population of He is in the ground state of the singlet system. The photoionization-recombination process (panels 2 and 3) is able to populate the triplet system significantly.

the two sets of levels are not radiatively coupled. For this reason, the lower energy level in the triplet system is a metastable one. At typical solar chromospheric conditions, the bulk of the Helium population is mainly concentrated in the 1S atomic ground level since the temperature is not high enough for populating the rest of the levels significantly. Thus, the insufficient population of the triplet system cannot account for the observed He I 10830 Å and 5876 Å features. It has been pointed out that the properties of the He I 10830 Å and D_3 multiplets depend mainly on the density and thickness of the chromosphere as well as on the incoming EUV irradiation from the corona that incides on the chromosphere (see Pozhalova 1988; Avrett et al. 1994; and earlier references therein). This EUV spectrum with $\lambda < 504$ Å ionizes Helium increasing the He II number density, which subsequently recombine with the free electrons populating in this way both singlet and triplet systems (Fig. 2 describes this process in 3 schematic steps). The excess population in the triplet energy levels is responsible for strengthening the He I 10830 Å and D_3 features.

The inclusion of coronal irradiance incident on the chromosphere was implemented in the RH code using the EUV flux given by Tobiska (1991). This author compiled data - provided by six different satellites- of the EUV coronal irradiance that reached the Earth in the period between 1962 and 1991. These data were used to evaluate the chromospheric illumination due to coronal sources, which is shown in Fig. 3.

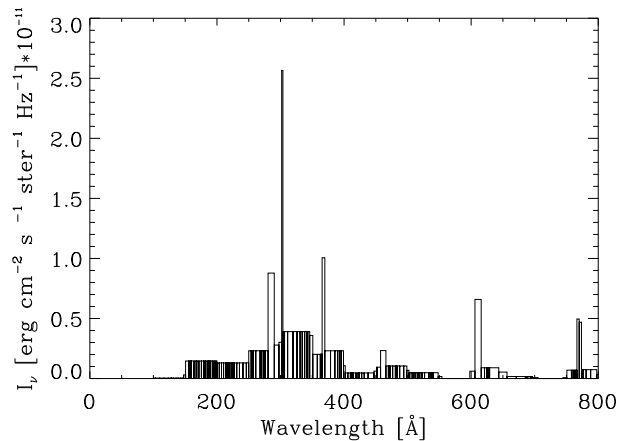


Fig. 3.— EUV flux incident on the chromosphere based on Tobiska (1991).

3. Results of the RT modeling calculations

Following the strategy described in the last section we carried out a thorough analysis of the sensitivity of the He I 10830 Å and D₃ emission profiles to the ionizing coronal irradiance. We will show, in particular, how off-limb observations of the He I 10830 Å multiplet can serve as a diagnostic tool for this EUV irradiance and discuss their use as a constraint for future atmospheric models.

3.1. He I 10830 Å and D₃ emission profiles

In a first approach to understand the off-limb emission of the lines of the 10830 Å and D₃ multiplets we compute the emergent profiles from the FAL-C model atmosphere. In order to calculate the non-LTE populations of He I and the emergent profiles we used a version of the RH code in 1D spherically symmetric geometry. We solved consistently the RT in spherical geometry and the SE equations to determine the populations at each height, and computed the emergent intensity profiles on a set of rays tangent to each spherical shell of the model atmosphere.

Fig. 4 represents the He I 10830 Å (left) and 5876 Å (right) profiles with increasing distance to the base of the photosphere² when the incident coronal irradiation takes its non-

²The height reference is set to be the level at which the optical depth -in the vertical direction- of the

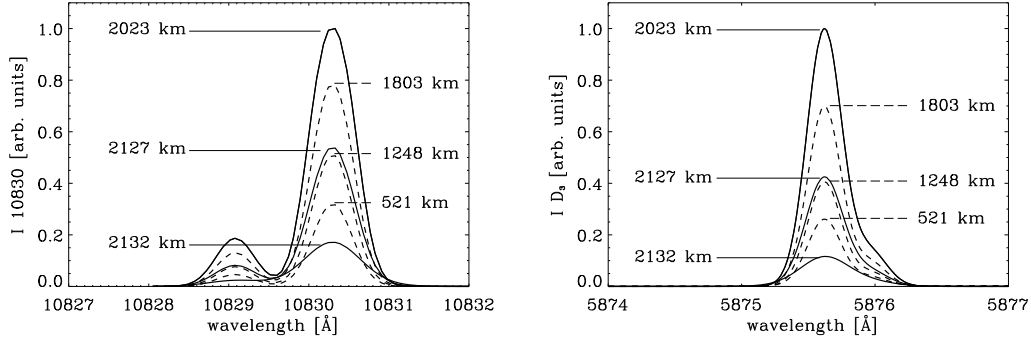


Fig. 4.— Off-the-limb He I 10830 Å (left) and D_3 5876 Å (right) emission profiles at different distances to the limb of the FAL-C semi-empirical model, when the nominal coronal irradiance has been applied to the system. Heights are given relative to the reference $\tau_{500} = 1$.

inal value (see Fig. 3). The lower height corresponds to the first profile seen in emission off the limb. In the outermost layers of the FAL-C model atmosphere, both multiplet transitions produce very little emission. As the distance to the limb decreases, the amplitude of the emergent profiles grows until it reaches a maximum around 2000 km. Below this point, the emission starts decreasing slowly until it turns into absorption inside the limb. The interpretation is as follows: the density in the outer layers of the atmosphere (at large distances from the limb) is so low that it cannot produce measurable emission profiles. As we go deeper into the atmosphere, the density increases quickly and so does the emission in the multiplets, until it reaches a maximum at a height of ~ 2000 km. The extinction of the EUV radiation as it travels inwards through the chromosphere leads to a reduction in the number of ionizations in the inner layers. Thus, the emission in the spectral lines of the He I 10830 Å and D_3 multiplets starts decreasing again because the PR mechanism cannot sustain the populations of the triplet system.

3.2. Dependence with coronal irradiance

One of the purposes of this investigation is to study the sensitivity of the emission profiles to the amount of coronal irradiance (CI).

The top panels of Fig. 5 show the 10830 Å (left) and D_3 (right) emergent profiles at

continuum at 500 nm equals unity, $\tau_{500} = 1$

the height of maximum emission (this is, 2023 km above $\tau_{500} = 1$) for four different values of the CI (0, 2, 5, and 10 times the nominal EUV spectrum). The tendency is clear: the stronger the CI, the greater the emission. As we shall see below, this is just a consequence of the increase in the population of the triplet levels with the CI. The lower panels of Fig. 5 represent the same intensity profiles when each of them is normalized to its maximum emission. The feature that strikes our attention most is the strong sensitivity of the relative amplitude of the blue component (I_B) of the He I 10830 Å multiplet to the strength of the incoming CI (lower left panel of Fig. 5). The ratio $\mathcal{R} = I_B/I_R$ of the amplitudes of the blue to red components of the multiplet changes substantially with the amount of ionizing radiation. This is an extremely interesting feature since it could provide a useful diagnostic tool for the incoming coronal irradiance in off-limb observations of the He I triplet. On the other hand, D_3 shows no observable relative changes among its spectral components in response to the ionizing radiation. We will see further on that this is just a natural consequence of the D_3 line not reaching enough optical thickness in these models to show a differential saturation behavior.

In order to understand the changes in the 10830 profiles shown in Fig. 5 let us see how the atomic populations behave in the absence/presence of the EUV ionizing spectrum. Fig. 6 shows the populations of the four J levels involved in the 10830 Å transitions (3S_1 , 3P_2 , 3P_1 and 3P_0 from left to right and top to bottom) as a function of height in the atmosphere, for five different values of the incoming CI (0, 1, 2, 5, and 10 times the nominal EUV flux). These plots clearly illustrate how the sole presence of CI dramatically changes the populations of these levels. Furthermore, the stronger the CI, the bigger this change. Note, however, that this sensitivity of the populations to the CI is only effective starting at a certain height (~ 1000 km) and that it keeps growing until it reaches the sharp density decrease that characterizes the transition region in the FAL-C model atmosphere. Below 1000 km, the extinction of the CI is such that it has no effect on the populations. It is interesting to notice that non-LTE effects play a significant role even in the absence of any coronal irradiance (compare the solid lines with the LTE results), but the ensuing overpopulation of the triplet levels above ~ 1500 km is insufficient to produce any significant optical thickness in the 10830 Å lines.

The left panel of Figure 7 shows the number of photoionizations per unit volume and time for increasing values of the coronal irradiance in the FAL-C model. Notice that the number of photoionizations that take place from the ground level decreases with height, proportionally to the population of this level - which follows the monotonical decrease of the atmospheric density profile. On the contrary, the amount of photoionizations taking place from the metastable level increases with height, due to the fact that the population of this level increases with height between about 600 and 2100 km, even in the LTE case (see Figure

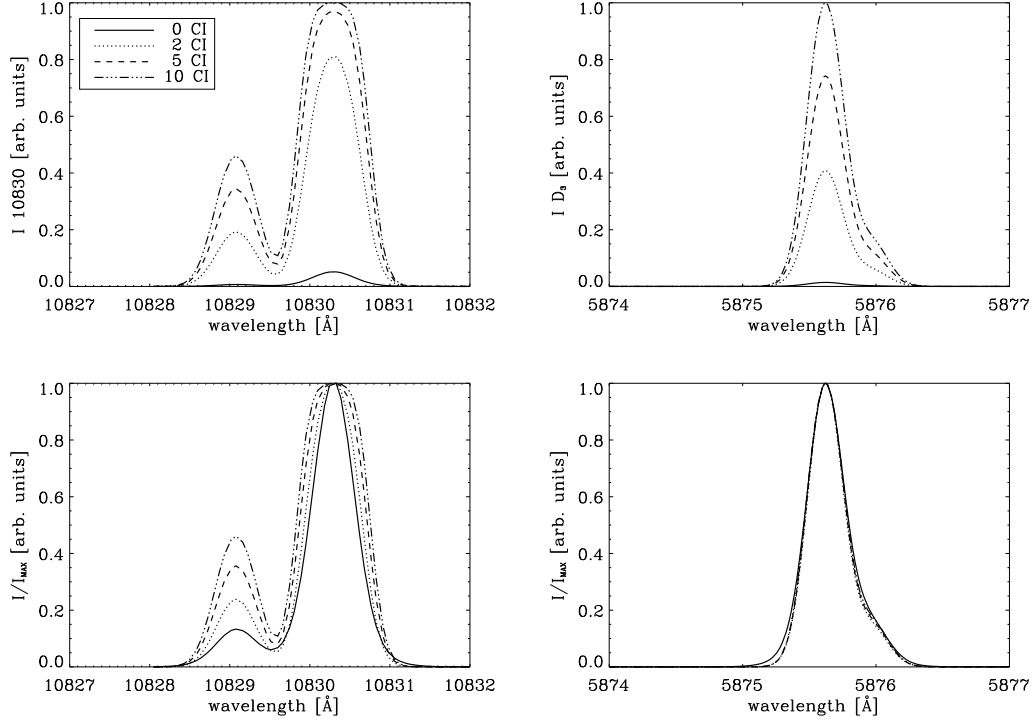


Fig. 5.— *Top*: Emission intensity profiles of He I 10830 Å (*left*) and D_3 (*right*) at a height of 2023 km above the $\tau_{500} = 1$ level for 4 different values of the incident coronal irradiance on the FAL-C atmospheric model. *Bottom*: Same profiles but normalized to their maximum. Note the sensitivity of the relative amplitudes of the blue and red components of He 10830 Å to the incoming CI.

6). The effect of the CI is such that it increases the population of the triplet levels at the expense of the ground level. This explains why, while the number of photoionizations from the metastable level grows with increasing CI, the number of photoionizations of the ground level becomes slightly smaller (due to the decrease in ground level population).

It is of some interest to point out that even with 10 times the nominal coronal value of the EUV flux, the number of photoionizations that take place from the ground level is ten orders of magnitude larger than that taking place from the metastable 3S_1 level. Even more interesting is to keep in mind what the right panel of Figure 7 illustrates - this is, that the number of bound-bound 10830 Å transitions per unit volume and time is way larger than the number of photoionizations from the same 3S_1 level. The same happens concerning the number of D_3 line transitions when compared to the number of photoionizations from their lower and upper J-levels.

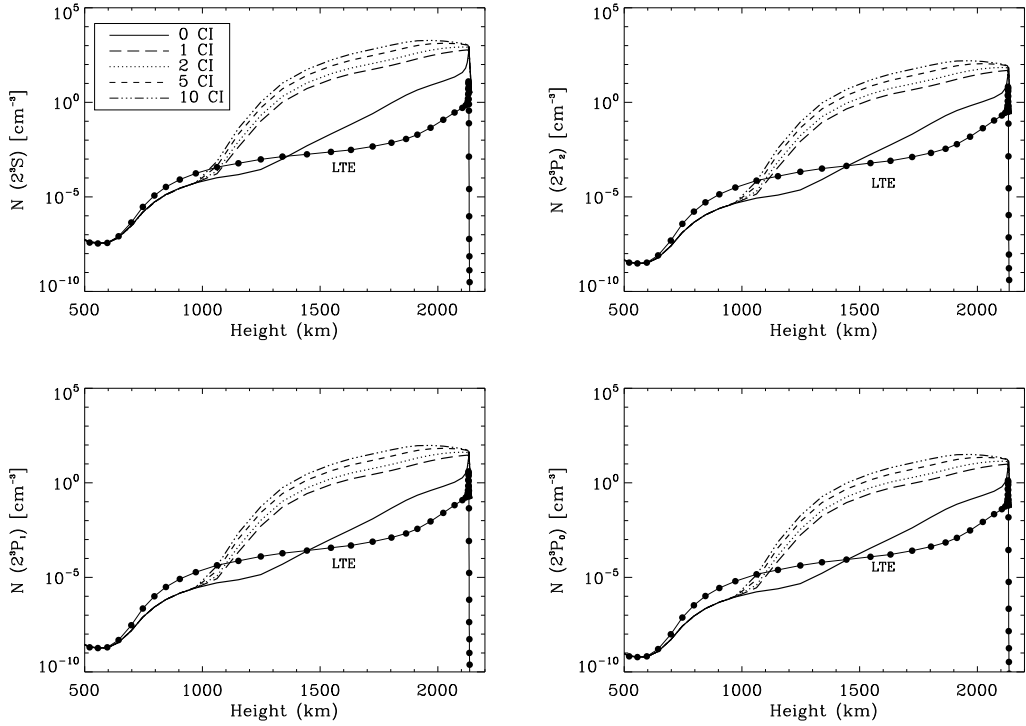


Fig. 6.— Populations of the energy levels involved in the 10830 Å transitions (from left to right and top to bottom: $3S$, $3P_2$, $3P_1$ and $3P_0$) as a function of height in the FAL-C model atmosphere (the reference level is $\tau_{500} = 1$). The populations were computed for 5 different values of the CI (0, 1, 2, 5 and 10 times its nominal value). Note that the sensitivity to the ionizing radiation starts at 1000 km above the base of the photosphere. The solid line with thick dots represents the populations in LTE, that, by definition, do not change with the coronal irradiance.

3.3. Interpretation in terms of the optical thickness of the line formation region

In a recent investigation, Trujillo Bueno et al. (2005) analyzed a set of spectropolarimetric observations of quiet Sun chromospheric spicules at $2''.5$ off the visible limb in the He I 10830 Å multiplet. In their first attempt, the authors tried to fit the emergent Stokes profiles ignoring the effects of radiative transfer (i.e., using the optically thin approximation). However, they found that they could not reproduce the emission of the blue component of the multiplet under this assumption. In a more realistic approach they were able to fit the emission profiles assuming a plane-parallel slab of constant physical properties and optical thickness τ , that accounts for the collective effect of having several spicules interposed along

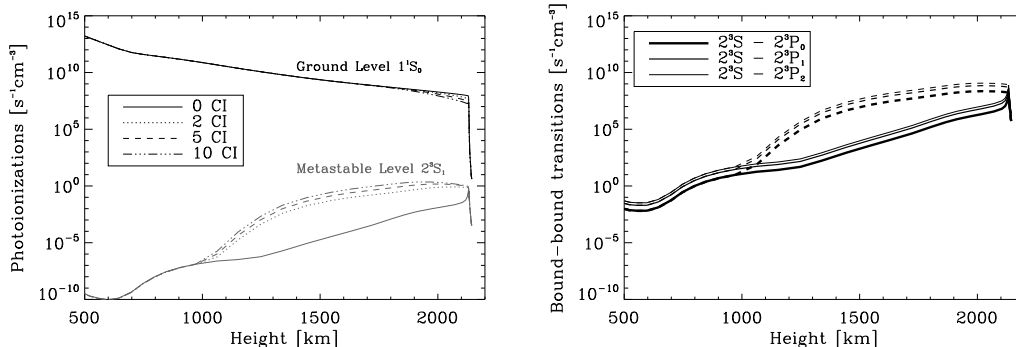


Fig. 7.— *Left*: Number of photoionizations in the FAL-C model atmosphere as a function of height. Black and grey show, respectively, the photoionizations from the ground and the metastable levels of the He I atom for 4 different values of the coronal irradiance. *Right*: Number of bound-bound transitions from the metastable level 2^3S to the three upper levels of the 10830 Å multiplet (represented with different line thickness) as a function of height and for 0 (*solid*) and 5 (*dashed*) times the nominal coronal irradiance.

the line of sight. With a value of $\tau_R = 3$ (of the optical thickness at the line center of the red blended component) the authors were able to reproduce the intensity ratio \mathcal{R} of the blue and red components of the multiplet, proving that radiative transfer effects are non-negligible.

The solid line in the right panel of Fig. 8 illustrates how the optical thickness of a slab of constant properties modifies the emission ratio \mathcal{R} of the two components of the 10830 Å multiplet. In the optically thin regime ($\tau_R < 1$), $\mathcal{R} = I_B/I_R$ takes a value around ~ 0.12 , which corresponds to the nominal ratio of oscillator strengths. For larger values of τ_R , this ratio \mathcal{R} increases with optical thickness until it reaches a saturation value of ~ 1 for $\tau_R \sim 30$. In this simple modeling, which is similar to that of Trujillo Bueno et al. (2005), the ratio \mathcal{R} is a function of τ_R in a wide range of optical thickness values. But what is the meaning and physical origin of this parametrization? Qualitatively, the relation between τ and the EUV coronal irradiation is easy to understand. The ionizing radiation modifies the population of the metastable level 2^3S , which in time is responsible for the optical thickness of the transition. But quantitatively, is this τ_R value chosen ad hoc by Trujillo Bueno et al (2005) to fit the profiles representative of the physical conditions of the solar corona and of the real integrated optical thickness along the line of sight?

To address this question we synthesized the He I 10830 Å profiles at a height of 2023 km above the base of the photosphere in the FAL-C model atmosphere, for different values of the incident coronal irradiance. Then, we computed the integrated optical depths along the line-of-sight (LOS) at the line center wavelength of the red blended component of the

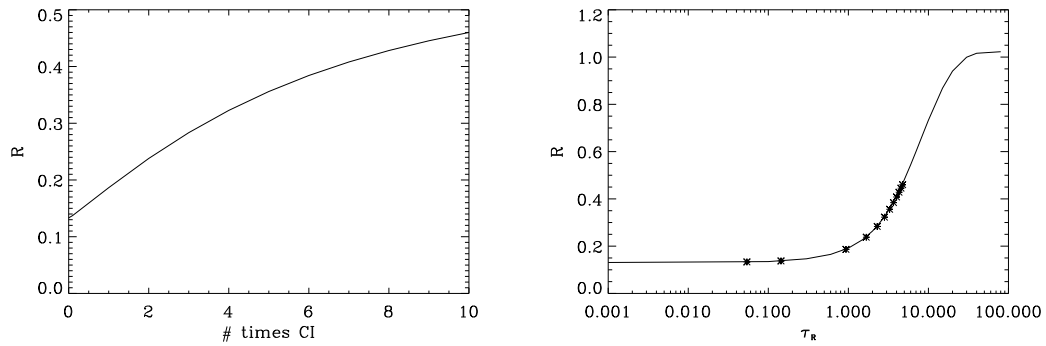


Fig. 8.— Influence of the coronal irradiance on the optical thickness and the ratio \mathcal{R} in the FAL-C model atmosphere. *Left:* \mathcal{R} as a function of the number of times the nominal CI that was applied in the calculations, for the emergent profiles at 2023 km above $\tau_{500} = 1$. *Right:* The solid line represents \mathcal{R} as a function of the optical depth at the line center of the red component of the multiplet as predicted by the optically thick slab modeling of Trujillo Bueno et al. (2005). Asterisks superposed to the solid line are the values obtained from the profiles simulated in the FAL-C model at the aforementioned height.

multiplet for each case. The left panel of Fig. 8 relates the measured ratio \mathcal{R} to the amount of inward ionizing radiation for a fixed distance to the limb. As expected, the stronger the CI, the greater the value of \mathcal{R} , although this relation is far from being linear and tends to saturate for very large values of the coronal irradiance. Asterisks superposed to the right panel of Fig. 8 show these computed values of \mathcal{R} as a function of the integrated optical depth along the line-of-sight. The excellent agreement with the constant-property slab modeling of Trujillo Bueno et al (2005) evidences that the ratio \mathcal{R} depends only on the integrated τ along the LOS, rather than on the spatial distribution of opacities.

When \mathcal{R} achieves values larger than the ratio of the oscillator strengths it means that the transitions are not in the optically thin regime anymore. In Figure 5 the reader can see that, while the normalized emission intensity profiles of the He I 10830 Å multiplet show a strong sensitivity to the incoming CI, He D₃, on the other hand, does not. This is a consequence of the distribution of populations in the triplet system of the He atom. The lower energy level of the 10830 Å transition is metastable, thus implying that its population is orders of magnitude larger than that of the rest of the triplet levels (see Figure 6). This produces a larger opacity in the 10830 Å multiplet that in turn affects the ratio \mathcal{R} . This is an interesting feature because, given the density profile of the atmosphere, this ratio should be a reliable tool for diagnosing the ionizing coronal irradiation, and viceversa.

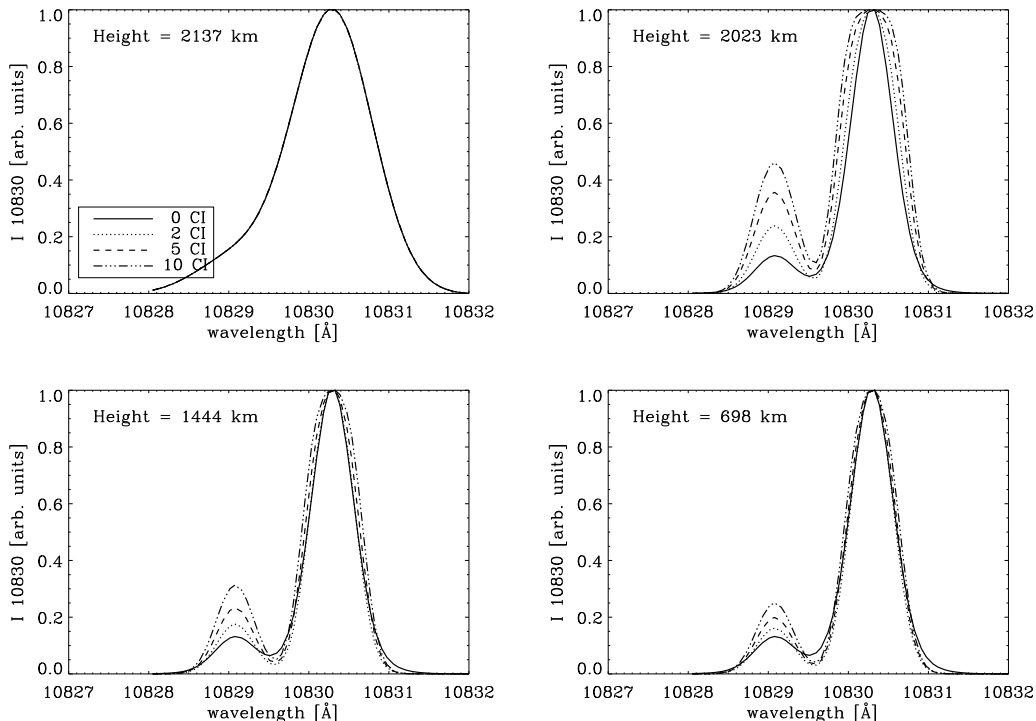


Fig. 9.— Normalized off-the-limb He I 10830 Å intensity profiles computed in FAL-C model atmosphere at different distances to the limb (from left to right and top to bottom, 2137 km, 2023 km, 1444 km and 698 km above $\tau_{500} = 1$). Each panel shows the intensity spectra for 0, 2, 5, and 10 times the nominal coronal irradiance).

3.4. Change of \mathcal{R} with height in various model atmospheres

The population of the metastable level changes with height, thus, the optical thickness in the 10830 Å transitions (and the relative amplitudes of the blue-to-red components of the multiplet, \mathcal{R}) should behave accordingly.

Fig. 9 illustrates the normalized emergent intensity profiles in the FAL-C model atmosphere at different heights above the limb (from left to right and top to bottom: 2137 km, 2023 km, 1444 km and 698 km above $\tau_{500} = 1$). Each panel shows the emission spectra for four values of the CI (0, 2, 5 and 10 times its nominal value). This figure proves how \mathcal{R} changes, not only with the amount of CI inciding on the chromosphere, but also with height in the atmosphere. This is an obvious consequence of the dependence of \mathcal{R} with the integrated optical depth along the ray path, and thus with the density. The top left panel of Fig. 9 corresponds to the emergent profiles from one of the outer-most layers of the FAL-C model. The three components of the multiplet appear completely overlapped due to the

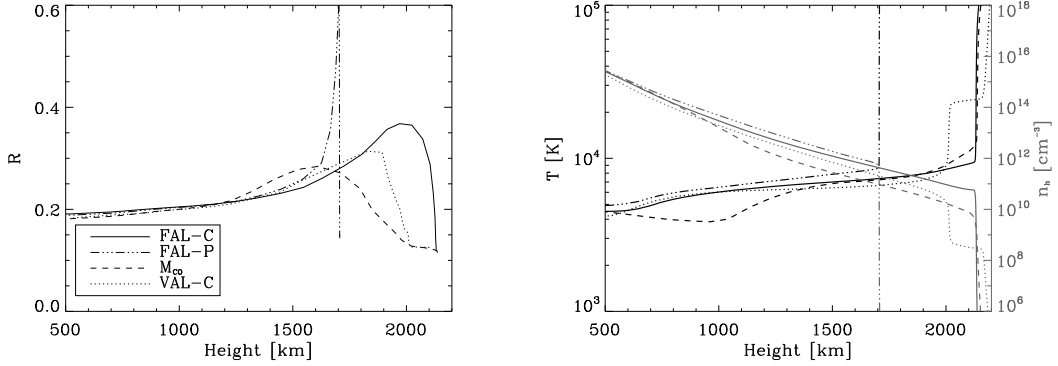


Fig. 10.— Comparison in 4 model atmospheres: FAL-C, FAL-P, VAL-C and the M_{CO} model of Avrett (1995). *Left*: Ratio \mathcal{R} of the blue-to-red components of the emergent He I 10830 Å intensity profiles as a function of height in the atmosphere when the applied CI takes 5 times its nominal value. *Right*: Hydrogen number density and temperature profiles as a function of height in the four model atmospheres.

large values of the microturbulent velocity ($\sim 8 - 10 \text{ km s}^{-1}$) at these heights. The widening effect that this contribution produces on the profiles is larger than the separation between the spectral components. The closer we get to the limb, the smaller the microturbulence and the easier it becomes to distinguish the red and blue components of the triplet. In the FAL-C model, within this range of CIs, the maximum emission (and ratio \mathcal{R}) is found at ~ 2023 km above $\tau_{500} = 1$, although in general, the stronger the CI, the lower in the atmosphere this would take place.

The top left panel of Fig. 10 shows the ratio \mathcal{R} as a function of height in four different standard model atmospheres (FAL-C, FAL-P, VAL-C and the M_{CO} model of Avrett 1995) when the applied CI flux takes five times its nominal value. The amplitudes of the blue and red components were extracted from a double gaussian fitting to the emergent intensity spectra. The higher layers of the atmosphere, where the overlap between the two components due to the microturbulence did not allow an unambiguous determination of \mathcal{R} , were excluded from the calculation (this is, above 1700 km in FAL-P and over 2100 km in VAL-C, FAL-C and the M_{CO} model of Avrett 1995). The very different behavior of the four curves is a consequence of the differences between the density profiles and the vertical extent of the model atmospheres. The right panel of Fig. 10 illustrates the density (*gray*) and temperature (*black*) stratifications in these four atmospheres. While FAL-P has a lower transition region (TR) boundary and a shallower chromosphere, all the other model atmospheres extend much higher and have thicker chromospheres. The lower height of the TR boundary in the FAL-P atmosphere combined with the effect of the strong ionizing radiation coming downwards

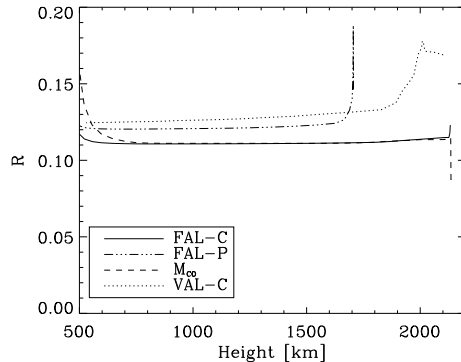


Fig. 11.— Comparison in 4 model atmospheres (FAL-C, FAL-P, VAL-C and the M_{CO} model of Avrett 1995) of the ratio \mathcal{R} as a function of height for the case with no coronal irradiance incident on the chromosphere. Note the effect of the temperature “plateau” of the VAL-C model in the region between 1900 and 2100 km. Also FAL-P shows a very localized peak produced by its sudden temperature increase at 1700 km above $\tau_{500} = 1$.

from the corona, shifts the region of formation of the He triplet towards lower heights in this model. Higher up, the medium becomes too rarified to produce enough opacity at the 10830 Å wavelength. The density profile of the M_{CO} model of Avrett (1995) in the transition region is not as steep as in FAL-C and FAL-P. For this reason, \mathcal{R} does not decrease as fast in the highest layers of the atmosphere.

The case for VAL-C is somewhat different. The presence of a temperature “plateau” at a height of 2100 km that defines a very thick transition region (of a couple hundred km) produces an increment of the population of the metastable level in this layer, even with no help from the ionizing radiation (cf. Andretta & Jones 1997). This is easy to see in Figure 11 where we represent the behavior of \mathcal{R} as a function of height in the four model atmospheres for the case of no coronal irradiance incident on the chromosphere. The temperature plateau and the thickness of the hot TR of VAL-C make possible a significant number of collisional excitations that lead to an over-population of the triplet system enough to produce a non-negligible optical thickness in the 10830 Å transition, but only for off-limb line-of-sights around 2100 km. Also FAL-P shows a very localized peak produced by the sudden increase in the temperature stratification at 1700 km above the level $\tau_{500} = 1$.

4. Concluding comment: a diagnostic tool of EUV coronal irradiance

Figure 10 shows the change of \mathcal{R} with height in four different model atmospheres. This variation is a very interesting feature since it sets a constraint on the thermodynamical structure of the chromosphere and the amount of ionizing coronal irradiance incident on it. \mathcal{R} is an observable that can easily be determined doing spectroscopic measurements of the He I 10830 Å multiplet. In fact, Sánchez-Andrade Nuño et al. (2007) made use of this theoretical prediction and have recently presented a series of observations of off-the-limb He I 10830 Å spectropolarimetric profiles aimed at the determination of \mathcal{R} . When comparing the observations with our radiative transfer modeling, they find that the theoretical behavior of the ratio \mathcal{R} agrees qualitatively with the observed one, although a quantitative comparison shows poor agreement. The density stratification and the limited vertical extent of the semiempirical model atmospheres considered in this paper are not adequate for spicule modeling. The fact that the solar chromosphere is very inhomogeneous on many scales and that spicules are small-scale intrusions of chromospheric matter into the hot corona, make it difficult for 1D models to reproduce off-limb observations.

The next step in this study should be to include in our RT modeling the spectral line polarization caused by the joint action of the Hanle and Zeeman effects, as done by Trujillo Bueno & Asensio Ramos (2007) within the framework of the above-mentioned slab model. New spectropolarimetric observations, at different positions above the solar limb with different levels of ionizing radiation (i.e. active regions and coronal holes) should be compared to the theoretical calculations to help constrain the atmospheric models and the physical processes that induce the formation of the He I 10830 Å and D₃ multiplets.

This research was partially funded by the Spanish Ministerio de Educación y Ciencia through project AYA2007-63881. The National Center for Atmospheric Research (NCAR) is sponsored by the National Science Foundation.

REFERENCES

- Andretta, V., Jones, H.P., 1997, ApJ, **489**, 375.
- Asensio Ramos, A., Trujillo Bueno, J., 2007, in *The Physics of Chromospheric Plasmas*, edited by P. Heinzel, I. Dorotovic and J. Rutten, ASP Conf. Series Vol **368**, 163.
- Avrett, E.H., Fontenla, J.M., Loeser, R., 1994, IAUS, **154**, 35.

- Avrett, E.H., 1995, in “Infrared tools for Solar Astrophysics: what’s next”, ed. J.R. Kuhn and M.J. Penn (Singapore: World Scientific), 303.
- Bianda, M., Ramelli, R., Trujillo Bueno, J., Stenflo, J., 2006, in “Solar Polarization Workshop 4”, eds. R. Casini and B.W. Lites; ASP Conf. Series Vol **358**, 454.
- Casini, R., López Ariste, A., Tomczyk, S., Lites, B., 2003, ApJ, **598**, L67.
- Centeno, R., Collados, M., Trujillo Bueno, J., 2006, ApJ, **640**, 1153.
- Fontenla, J.M., Avrett, E.H., Loeser, R., 1990, ApJ, **355**, 700.
- Fontenla, J.M., Avrett, E.H., Loeser, R., 1991, ApJ, **377**, 712.
- Fontenla, J.M., Avrett, E.H., Loeser, R., 1993, ApJ, **406**, 319.
- Lagg, A., Woch, J., Krupp, N., Solanki, S.K., 2004, A&A, **414**, 1109.
- Landi Degl’Innocenti, E., 1982, Solar Physics, **79**, 29.
- Landolt-Börnstein, Volume 2, Astronomy and Astrophysics, subvolume b, Stars and Star clusters, 1982, Springer-Verlag, (98-100).
- Leroy, J.L., Bommier, V., Sahal-Bréchet, S., 1983, Solar Physics, **83**, 135.
- Lin, H., Penn, M.J., Kuhn, J.R., 1998, ApJ, **493**, 978.
- López Ariste, A., Casini, R., 2005, A&A, **436**, 325.
- Merenda, L., Trujillo Bueno, J., Landi Degl’Innocenti, E., Collados, M., 2005, ApJ, **642**, 544.
- Pozhalova, zh. A., 1988, Sov. Astron., 65(5).
- Ramelli, R., Bianda, M., Merenda, L., Trujillo Bueno, J., 2006a, in “Solar Polarization Workshop 4”, eds. R. Casini and B.W. Lites, ASP Conf. Series Vol. **358**, 448.
- Ramelli, R., Bianda, M., Trujillo Bueno, J., Merenda, L., Stenflo, J.O., 2006b, in “Solar Polarization Workshop 4”, eds. R. Casini and B.W. Lites, ASP Conf. Series Vol. **358**, 471.
- Rüedi, I., Solanki, S.K., Livingston, W., 1995, A&A, **293**, 252.
- Rybicki, G.B., Hummer, D.G., 1991, A&A, **245**, 171.

- Rybicki, G.B., Hummer, D.G., 1992, *A&A*, **262**, 209.
- Tobiska, W. Kent, 1991, *Journal of Atmospheric and Terrestrial Physics*, **53**, 1005.
- Sánchez-Andrade Nuño, B., Centeno, R., Puschmann, K.G., Trujillo Bueno, J., Blanco Rodríguez, J., Kneer, F., 2007, *A&A Letters*, in press.
- Seaton, M.J., 1962, *Proc. Phys. Soc. London*, **79**, 1105.
- Socas-Navarro, H., Elmore, D., 2005, *ApJ*, **619**, 195.
- Socas-Navarro, H., Trujillo Bueno, J., 1997, *ApJ*, **490**, 383.
- Trujillo Bueno, J., Asensio Ramos, A., 2007, *ApJ*, **655**, 642.
- Trujillo Bueno, J., Landi Degl’Innocenti, E., Merenda, L., Collados, M., Manso Sainz, R., 2002, *Nature*, **415**, 403.
- Trujillo Bueno, J., Merenda, L., Centeno, R., Collados, M., Landi Degl’Innocenti, E., 2005, *ApJ*, **619**, 191.
- Van Regemorter, H., 1962, *ApJ*, **136**, 906.
- Vernazza, J.E., Avrett, E.H., Löser, R., 1981, *ApJS*, **45**, 635.